

Preparation and Properties of Al_2O_3 /Steel-epoxy Laminated Composites

LI Wei-Xin, BAI Ming-Min, LU Ying, RAO Ping-Gen

(School of Materials Science and Engineering, South China University of Technology, Guangzhou 510640, China)

Abstract: A series of Al_2O_3 /steel-epoxy laminated composites were prepared by using epoxy resin adhesive as binder via a simple process in a leaky mould at a pressure of 5 MPa. The results indicate that the interfaces of Al_2O_3 /epoxy and steel/epoxy are joined tightly, and the laminated composites have much higher fracture toughness, impact toughness and energy consumption than the Al_2O_3 monolith, as well as having a close strength to Al_2O_3 . The crack propagation behavior indicates that the improvement of toughness and energy consumption attribute to the mechanisms of crack blunting and arresting, crack bridging, interface debonding, ductile deformation of steel-epoxy mesh layer.

Key words: laminated composites; alumina; interfaces; steel-epoxy; mechanical properties; toughening mechanism

Laminated composites have received more and more attention in the past few decades since Clegg^[1] prepared SiC/C laminates in 1990. Combining a strong layer and weak layer (or a hard layer and tough layer) is one of the popular concepts for laminated composites' design. The strong layers are usually thick using generally various ceramics with good mechanical properties, including Al_2O_3 ^[2], B_4C ^[3], ZTA^[4], Si_3N_4 ^[5], while the weak layers (or tough layers) are usually thin such as BN^[5], SiC^[6], W^[7], Ni^[2] and epoxy^[8]. By far most popular manufacturing processes for laminated composites require several steps. First, ceramic powders used for strong layers are made into thin sheets by methods such as tape casting^[3], centrifugal casting^[9], dough rolling^[11]. Then, the materials used for weak layers are also made into thin sheets by the same methods, or stick to the strong layers by depositing, dipping or spraying. Finally, the sheets overlapped together in a certain order are pressed and sintered by hot-pressing^[4] or spark plasma sintering^[10]. However, the processes mentioned above require sophisticated equipment like hot-pressing furnace and strict conditions such as high temperature, high pressure, strong electric current, and so on. Moreover, the processes are expensive and some of them may lead to environmental pollution.

In this study, a simple technology of mould pressing was used to fabricate a hybrid laminated composites with high strength, high fracture toughness, and high energy consumption by using alumina ceramic, steel mesh, and epoxy resin adhesive. No sophisticated equipments and experimental situation were adopted in the whole process except a set of mould and a compressor. The laminated composites have good mechanical properties, especially

having much energy consumption during fracture, which have a good prospect in fields where requiring energy absorbing such as in anti-impact applications.

1 Experimental procedure

Al_2O_3 slices (95 alumina, 0.635 mm×60 mm×70 mm) were purchased from Zhuhai Yueke Jinghua Electronic Ceramics Company with the bending strength of 300 MPa. Steel mesh was commercially obtained from Guangzhou Zhida Nets Co., Ltd. Epoxy resin adhesive was purchased from Nanbao Resins (China) Co., Ltd., which mainly consists of epoxy resin and polyamide. Several series of the laminated ceramic composites were prepared, named as A/A, A/400, A/300, A/250, A/200, A/150, A/120, A/80, and A/60. A denotes as alumina and the number denotes as steel mesh. For example, A/200 means the composites obtained by alternately superimposing one layer of alumina and one layer of 200# steel mesh.

Based on the previous work^[11-13], the specimens are decided to be fabricated by 7 layers of Al_2O_3 and 6 layers of steel-epoxy. As shown in Fig. 1, the manufacturing steps taken to prepare the laminated ceramic composites include: (1) epoxy resin was first mixed thoroughly with hardener in appropriate proportion, and then put into vacuum oven for 10–20 min to remove the bubbles; (2) the mixed adhesive was applied to surface of Al_2O_3 slices and steel mesh, then stack them one by one; (3) the composites made in Step 2 were put into a leaky mold, and then pressed at a pressure of 5 MPa for 2 h; (4) open the mould and take the sample out. The samples were exposed to air for 5–10 d to ensure the resin cured completely before testing.

Received date: 2012-11-27; Modified date: 2012-12-26; Published online: 2013-01-30

Foundation item: Science and Technology Program of Guangdong Province of China (2010B090400330)

Biography: LI Wei-Xin (1980–), male, candidate of PhD. E-mail: 38058449@qq.com

Corresponding author: RAO Ping-Gen, professor. E-mail: pgrao@scut.edu.cn

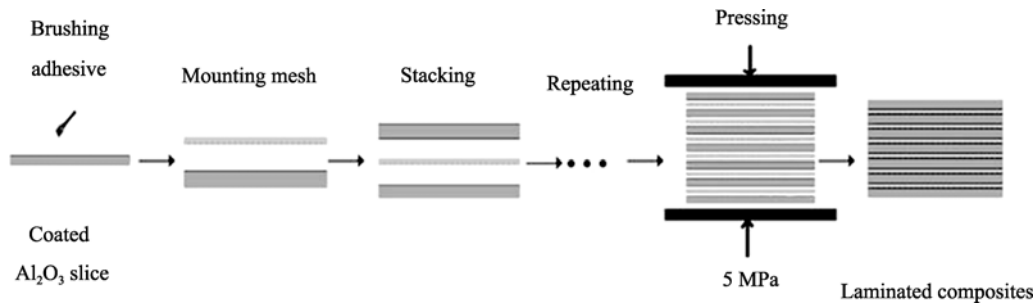


Fig. 1 Preparation process of laminated composites

The density of the laminated composites was measured by the Archimedes method. The Young modulus was determined by the slope of load-displacement curve within the strain of 0.03%–0.10% using a clip-on extensometer (2630-100, Instron, USA). The macroscopic and microstructural characterization was performed by an optical microscope (XTZ-E, Shanghai, China) and a scanning electron microscope (EVO18 Special Edition, Zeiss, Germany). Three-point bending strength was tested using a 30 mm span and a crosshead speed of 0.5 mm/min at room temperature (5567, Instron, USA). The fracture toughness (K_{IC}) was evaluated by the single-edge notched beam (SENB) technique with a 30 mm span and a crosshead speed of 0.05 mm/min, as shown as Fig. 2, the straight edge notch was introduced at the center part of the test bar by a cutting machine with a 150- μm -wide diamond blade from the Al_2O_3 layer to epoxy-steel layer, and the notch tip terminates at Al_2O_3 layer. The value of $K_{IC}(\text{MPa}\cdot\text{m}^{1/2})$ is given by:

$$K_{IC} = \frac{3FL}{2Bw^2} \sqrt{a} \left(1.93 + 3.07\left(\frac{a}{w}\right) + 13.66\left(\frac{a}{w}\right)^2 - 23.98\left(\frac{a}{w}\right)^3 + 25.8\left(\frac{a}{w}\right)^4 \right) \quad (1)$$

Where, F is the maximum load (N) before the notched specimens break, L is the span (mm), B is the width (mm), w is the thickness (mm), a is the notch size (mm).

The impact toughness (α_k) was evaluated by pendulum impact test. Each five bars were used to get the average values of the strength, fracture toughness and impact

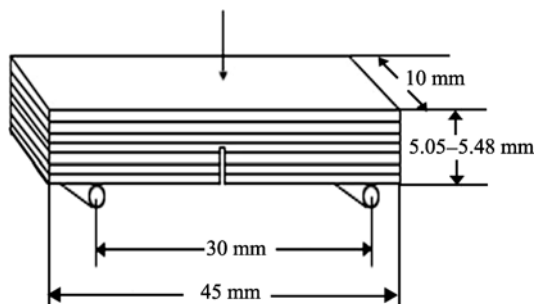


Fig. 2 Specimens dimension and loading pattern during fracture toughness test

toughness, respectively. The energy consumption was calculated from the area under the load-displacement curve after the three-point bending strength test.

2 Results and discussion

2.1 Structure of Al_2O_3 /steel-epoxy composites

Figure 3 shows the SEM images of the A/200. The macrostructure (Fig.3(a)) shows that the Al_2O_3 layers are bright and thick, while the steel-epoxy layers are dark and thin. The structure of steel mesh is plain weave, as shown in Fig. 3(b), and the mesh gaps are fully filled with epoxy. The interfaces of Al_2O_3 /epoxy and steel/epoxy are shown in Fig. 3(c) and Fig. 3(d). It is observed that the interface between Al_2O_3 and epoxy is clear and straight, and the interface between steel wire and epoxy is circular. No obvious defects are observed in the interfaces.

The steel mesh, used as reinforcement, can also control the thickness of steel-epoxy by choosing different number of mesh. The epoxy adhesives, used as matrix in steel-epoxy layer, can not only bond the Al_2O_3 and the steel-epoxy together, but also play the role of absorbing energy due to its excellent plastic deformation ability. The diameter of the steel wires for 400#, 300#, 250#, 200#,

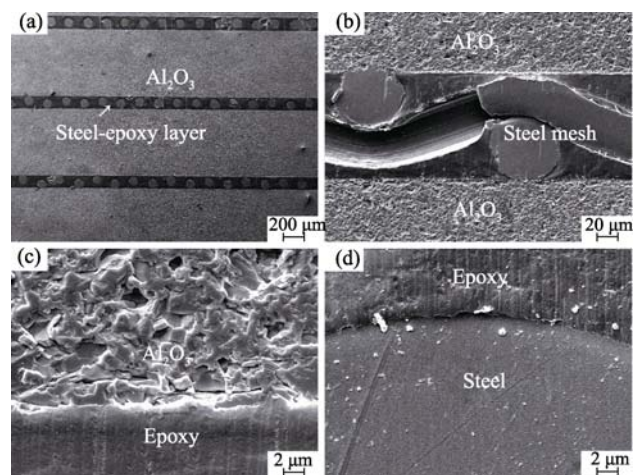


Fig. 3 SEM images of the laminated composites

(a) Low magnification; (b) Mesoscale image; (c) Interface of Al_2O_3 /epoxy; (d) Interface of steel/epoxy

150#, 120#, 80# and 60# meshes are about 59, 72, 80, 85, 105, 128, 146 and 150 μm , respectively. The thickness of the steel-epoxy layers for 400#, 300#, 250#, 200#, 150#, 120#, 80# and 60# meshes are about 90, 110, 125, 131, 162, 180, 195 and 206 μm , respectively.

2.2 Load-displacement curves and energy consumption of $\text{Al}_2\text{O}_3/\text{steel-epoxy}$ composites

Figure 4(a) shows the typical load-displacement curve of $\text{Al}_2\text{O}_3/\text{steel-epoxy}$ laminated composites, where σ_i ($i=0\sim n+1$) is the peak loading value, and the S_i ($i=0\sim n$) is the area integral of the solid segment and x axis. When crack initiates at surface of Al_2O_3 layer and grows to another side of specimen, all the Al_2O_3 layers crack, and σ_0 is the peak load value of this stage. However, the specimen does not break into pieces owing to the bridging of steel-epoxy layer. The specimen can still bear a certain of loading until all the steel-epoxy layers break off. σ_i ($i=2\sim n+1$) is the loading value when the i -th steel-epoxy layer breaks. So, the segment $\sigma_0\sim\sigma_1$ corresponds to the breaking of all the Al_2O_3 layers and the S_0 is the energy consumption before σ_1 . The segment $\sigma_i\sim\sigma_{i+1}$ ($i=1\sim n-1$) correspond to the breaking of i -th steel-epoxy layer and S_i ($i=1\sim n-1$) is the energy consumption between σ_i and σ_{i+1} .

W is defined as the total energy consumption throughout the fracturing process of specimen. W_a is defined as the energy consumption before σ_1 when all the Al_2O_3 layers crack. W_{se} presents the total energy consumption between σ_1 and σ_{n+1} , mainly caused by broken of steel-epoxy layers. η is defined as the ratio between W_{se} and W_a . W , W_a , W_{se} and η can be given by

$$W = W_a + W_{se} \quad (2)$$

$$W_a = S_0/A \quad (3)$$

$$W_{se} = (S_0 + S_1 + \dots + S_n) \quad (4)$$

$$\eta = W_{se}/W_a \quad (5)$$

Where, A is the cross-sectional area of specimens. According to formula (2) to (5):

$$\eta = (S_1 + S_2 + \dots + S_n)/S_0 \quad (6)$$

As shown in Fig. 4(b), η decreases rapidly with the number of mesh less than 200 and keeps stable after 200. It is suggested that the sharp fall of η is mainly because of the larger variation of steel wires' diameter before 200.

The number of steel mesh will also have influence on the fracture of Al_2O_3 layer. The earlier parts of the load-displacement curves and the energy consumption of the A/200, A/150 and A/120 laminated composites are plotted in Fig. 5. The solid lines show the load-displacement curves and the dotted lines are the corresponding energy consumption obtained by area integral of the solid line and x axis. The load-displacement curves are nearly linear up to the peak value for A/200 and A/150, however, the curve of A/120 shows some 'pop-in' as rising. It is suggested that the different representations of 'pop-in' are because of the different thickness of epoxy-steel mesh layer. The end parts of the load-displacement curves are platforms, which are considered as the residual load of epoxy-steel mesh layer after all the Al_2O_3 broke. The residual strength according to the platform is calculated to be 60, 55 and 38 MPa, respectively.

As a result, multiple fractures, considered to be developed by the confinement and the shear process of epoxy-steel mesh layer, are observed in Fig. 6(a) to Fig. 6(c). According to model of ceramic/superplastic laminates created by Deng^[14], there exist a residual stress due to the confinement by epoxy-steel mesh layer and a shear-accumulated stress by the shear process of superplastic flow which originates from the difference in strain rate. When an Al_2O_3 layer breaks, although the stress releases temporarily, new stress will emerge in the broken Al_2O_3 layer because the bridging epoxy-steel layer can still transfer the stress to Al_2O_3 layer when the load in crease. When the total stress exceeds the critical fracture stress, another new crack occurs in the broken Al_2O_3 layer, and multiple fractures happen after some repeating of the cracks mentioned above. From Fig. 6(a) to Fig. 6(c), it can

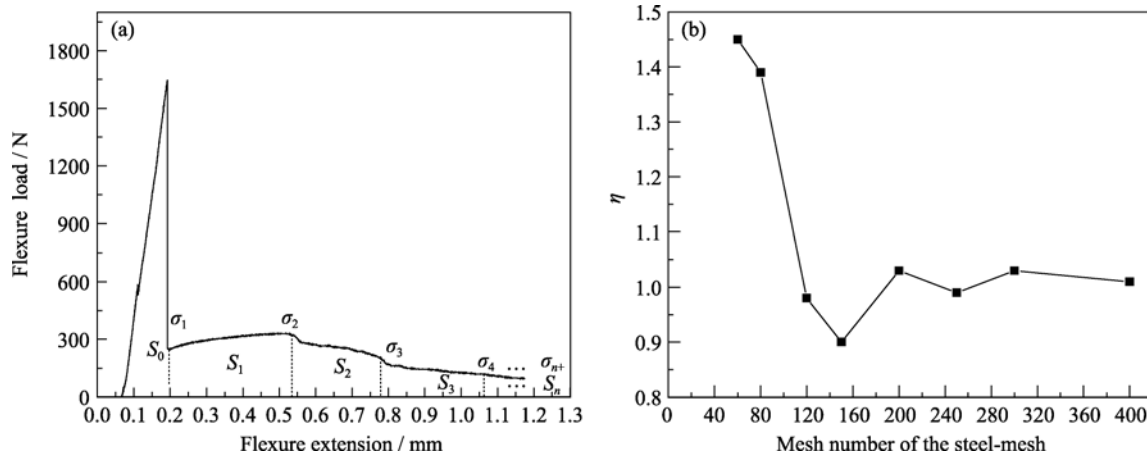


Fig. 4 (a) The typical load-displacement curve of $\text{Al}_2\text{O}_3/\text{steel-epoxy}$ laminated composites; (b) η vs mesh number of steel mesh

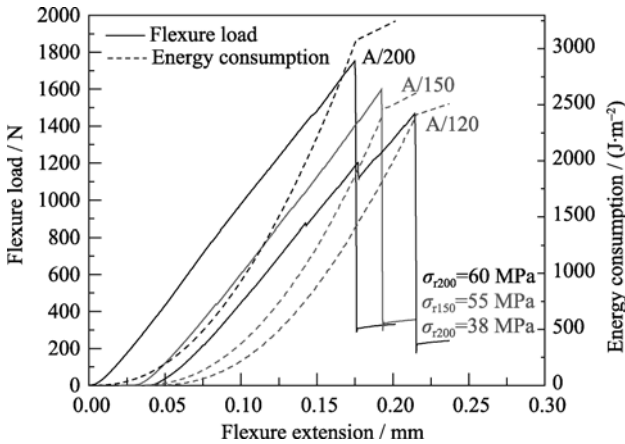


Fig. 5 The earlier parts of the load-displacement curves and the energy consumption for A/200, A/150 and A/120

also be seen that there tend to be more cracks when the thickness of epoxy-steel mesh layer increases, because the stress in Al_2O_3 layer increase with the thickness of epoxy-steel mesh layer.

2.3 Mechanical properties of Al_2O_3 /steel-epoxy composites

Table 1 summarizes the mechanical properties of Al_2O_3 monolith and the laminated composites. It is concluded that A/200 have better properties. The density of A/200 is 3.57 g/cm^3 , and the Young modulus is only 162 GPa. The densities of all the laminated composites are lower than that of alumina monolith, and both the density and the Young modulus decrease with reducing of the number of steel mesh. Decreasing of the density can be interpreted by the rule of mixture, while the Young Modulus is much lower than the value calculated by the rule of mixture. It is considered that the interfaces of different materials and plastic deformation of steel-epoxy layer are the main reasons why Young Modulus has a large drop. The bending strength of A/200 is 303 MPa, which is nearly equal to that of the Al_2O_3 monolith. The fracture toughness of A/200 reaches about $14.5 \text{ MPa}\cdot\text{m}^{1/2}$ which is about 4 times of that of the Al_2O_3 monolith, and the total energy con-

sumption(W) of A/200 is up to 6087 J/m^2 , which is about hundreds of times of Al_2O_3 monolith. In addition, the impact toughness of the sample is 8.5 kJ/m^2 .

The composites of A/A have a higher density and Young modulus, however, its bending strength is considerably lower than that of monolithic alumina and the rest of laminates. It is supposed that the decreasing of bending strength is attributed to the residual stresses in laminates. For A/A and other laminates, there exist a compression stress in Al_2O_3 layers and a tensile stress in epoxy layers or steel-epoxy layers. The epoxy layer of A/A is only about several micron, which is considerably thinner than that of other laminates. Therefore, the compression stress in Al_2O_3 layer of A/A is lower, while the tensile stress in epoxy layer is higher than the rest of laminates. The compression stress in Al_2O_3 layer is helpful, while the tensile stress in epoxy or steel-epoxy is harmful to the bending strength. Moreover, the fracture toughness, impact toughness and energy consumption of A/A are all lower than that of the rest of laminates. In other words, the introduce-

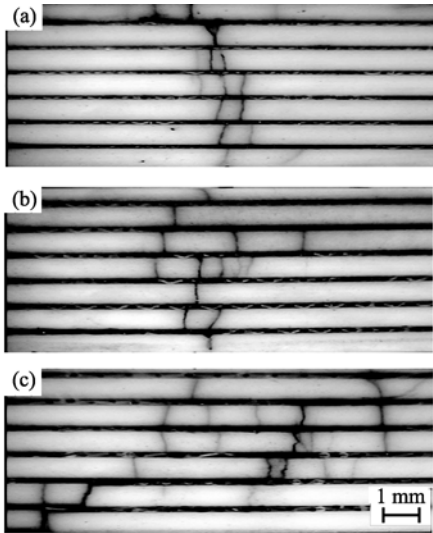


Fig. 6 The optical micrograph showing the corresponding crack propagation (a) A/200; (b) A/150; (c) A/120

Table 1 Mechanical properties of Al_2O_3 monolith and various laminated composites

Samples	Density, $\rho/(\text{g}\cdot\text{cm}^{-3})$	Young modulus, E/GPa	Bending strength, σ/MPa	Fracture toughness, $K_{\text{Ic}}/(\text{MPa}\cdot\text{m}^{1/2})$	Energy consumption		Impact toughness, $\alpha_k/(\text{kJ}\cdot\text{m}^{-2})$
					$W_a^*/(\text{J}\cdot\text{m}^{-2})$	$W/(\text{J}\cdot\text{m}^{-2})$	
Al_2O_3	3.74	360	300 ± 44	—	—	0	—
A/A	3.65	188	199 ± 16	10.1 ± 1.2	1500 ± 200	0	4.2 ± 0.5
A/200	3.57	162	303 ± 16	14.5 ± 0.6	3000 ± 300	6087 ± 424	8.5 ± 0.9
A/150	3.52	148	286 ± 28	14.2 ± 0.5	2600 ± 260	5740 ± 335	9.1 ± 0.9
A/120	3.43	129	260 ± 30	14.3 ± 0.6	2334 ± 280	5508 ± 387	10.6 ± 1.0

* W_a is the energy consumption when all Al_2O_3 layers crack

tion of steel mesh enhances the mechanical properties of the laminated Al_2O_3 based composites.

Figure 7 shows the influence of steel mesh on the mechanical properties of laminated composites. The bending strength increases with the number of mesh. The fracture toughness reaches maximum value at 200 mesh, and increases with the number of mesh before 200 and decrease after 200. The total energy consumption increase with the number of mesh before 200 and changes little after 200. The impact toughness decreases with the number of mesh increasing.

2.4 Crack propagation and mechanisms of the $\text{Al}_2\text{O}_3/\text{steel-epoxy}$ composites

Figure 8 shows the crack initiation and propagation during three-point bending test of the notched composites sample. According to the model of the three-point bending test, the residual stress in the middle part of the sample is largest. As Fig. 8(a) shown, when crack initiates from some defects of notched surface in the middle part of the sample and grows quickly to the interface of Al_2O_3 and epoxy-steel mesh layer, cracks are arrested because of crack tip shielding caused by the epoxy-steel layer. With a further applied load increasing in order to maintain the

loading rate imposed during testing, another crack initiates at neighboring surface of Al_2O_3 layer and propagates to the deeper adjacent interface of Al_2O_3 and epoxy-steel mesh layer before being arrested. The repeating of the process builds up a continuous macroscopic crack with the epoxy-steel layer remaining intact, as well as the mentioned multi-cracks above sometimes.

Some mechanisms are considered to enhance the ability of absorbing energy when the laminated composite fractures such as crack blunting and arresting, crack bridging, interface debonding, ductile deformation of epoxy-steel layer and so on. That crack tip is blunted and arrested at the interface of $\text{Al}_2\text{O}_3/\text{epoxy}$, and the epoxy-steel layer plays a bridge role to connect the two neighboring cracks, as shown in Fig. 8(d), leads to the resistance to crack propagation. Deforming of steel and epoxy can be observed in Fig. 8(b) and Fig. 8(d), which dissipate the stress concentration in epoxy-steel layer to increase the toughness of the laminated composites. The debonding of epoxy/ Al_2O_3 interfaces and epoxy/steel interfaces, as shown in Fig. 8(c) and Fig. 8(d), plays a similar role. These mechanisms work cooperatively to enhance the toughness of the laminated composites.

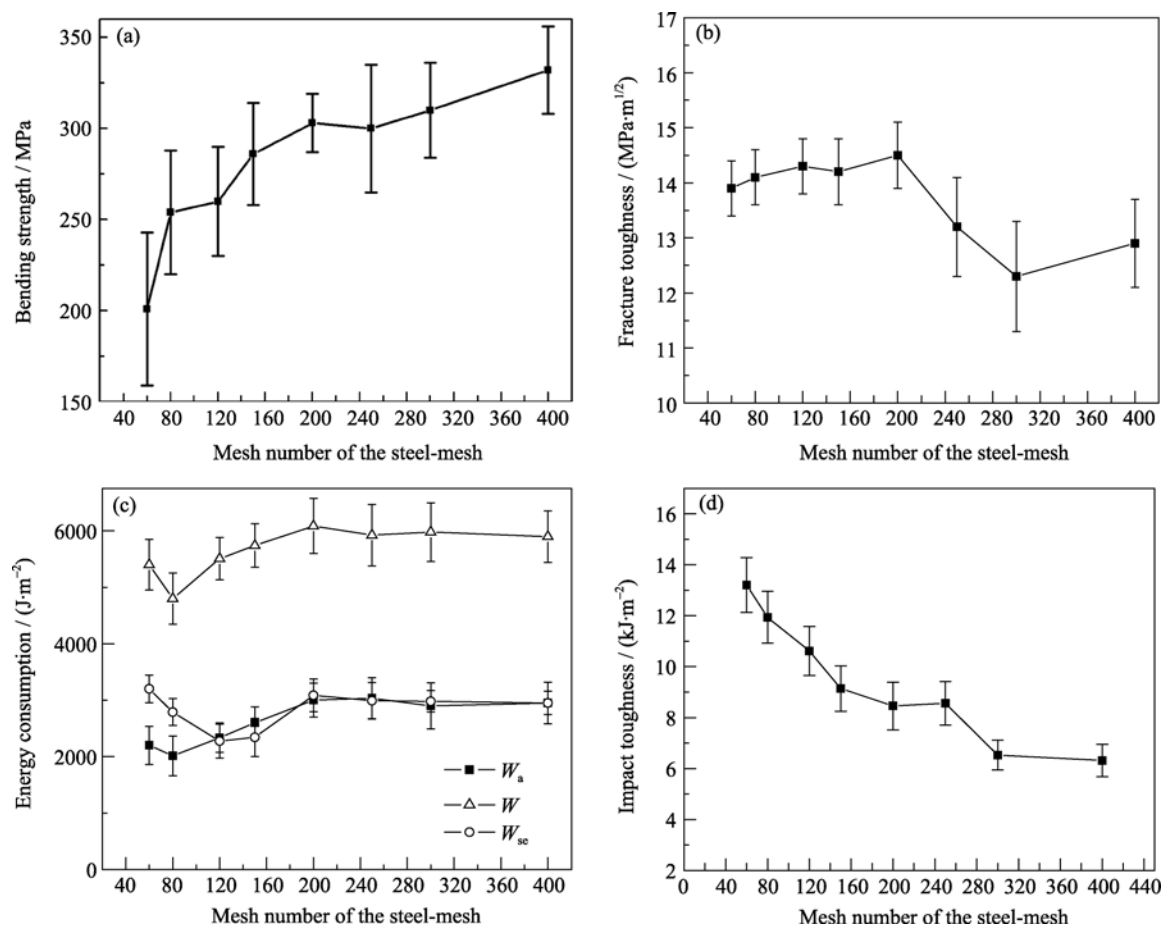


Fig. 7 Influences of steel mesh on the mechanical properties of laminated composites
(a) Bending strength; (b) Fracture toughness; (c) Energy consumption; (d) Impact toughness

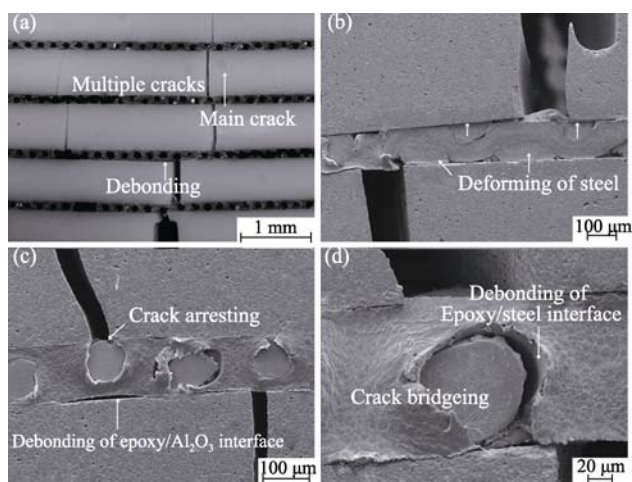


Fig. 8 Crack initiation and propagation in notched laminated composite during three-point bending test

3 Conclusion

Laminated Al_2O_3 based composites with steel mesh and epoxy as interlayer were fabricated by a simple process. The interfaces of Al_2O_3 /epoxy and steel/epoxy are joined tightly. The strength of the laminated A/200 is 303 MPa, which is nearly equal to that of the aluminum monolith. The fracture toughness, impact toughness and energy consumption is $14.5 \text{ MPa}\cdot\text{m}^{1/2}$, 8.46 kJ/m^2 and 6087 J/m^2 , respectively. All of them are much higher than that of the aluminum monolith. The typical load-displacement curves of the laminates have features of “pop-in” and platform, and the corresponding crack propagation exhibits the characteristic of multi-cracks growing. The improvement of toughness and energy consumption attributes to some mechanisms such as crack blunting and arresting, crack bridging, interface debonding, ductile deformation of epoxy-steel mesh layer.

References:

- [1] Clegg W J, Kendall K, Alford N M, *et al.* A simply way to make tough ceramics. *Nature*, 1990, **347**: 455–457.
- [2] ZUO Kai-Hui, JIANG Dong-Liang, LIN Qing-Ling. Mechanical properties of $\text{Al}_2\text{O}_3/\text{Ni}$ laminated composites. *Materials Letters*, 2006, **60**(9/10): 1265–1268.
- [3] Tariolle S, Reynaud C, Thevenot F, *et al.* Preparation, microstructure and mechanical properties of SiC-SiC and $\text{B}_4\text{C-B}_4\text{C}$ laminates. *Journal of Solid State Chemistry*, 2004, **177**(2): 1487–1492.
- [4] Bermejo R, Baudin C, Moreno R, *et al.* Processing optimisation and fracture behaviour of layered ceramic composites with highly compressive layers. *Composites Science and Technology*, 2007, **67**(9): 1930–1938.
- [5] LI Cui-Wei, WANG Chang-An, HUANG Yong, *et al.* Effects of sintering aids on the microstructure and mechanical properties of laminated $\text{Si}_3\text{N}_4/\text{BN}$ ceramics. *Materials Letters*, 2002, **57**(22/23): 336–342.
- [6] SHE Ji-Hong, Takahiro Inoue, Kazuo Ueno. Multilayer $\text{Al}_2\text{O}_3/\text{SiC}$ ceramics with improved mechanical behavior. *Journal of European Ceramic Society*, 2000, **20**(11): 1771–1775.
- [7] GAO Yong-Yi, ZHENG Shi-Yuan, ZHU Kai-Cheng. Analysis of mechanical properties and SEM for laminated SiC/W composites. *Materials Letters*, 2001, **50**(5/6): 358–363.
- [8] ZHAO Su, ZHANG Ji-Zhong, ZHAO Shi-Qi, *et al.* Effect of inorganic-organic interface adhesion on mechanical properties of Al_2O_3 /polymer laminate composites. *Composites Science and Technology*, 2003, **63**(7): 1009–1014.
- [9] Lucchini E, Sbaizero O. Alumina/Zirconia multilayer composites obtained by centrifugal consolidation. *Journal of European Ceramic Society*, 1995, **15**(10): 975–981.
- [10] LI Cui-Wei, HUANG Yong, WANG Chang-An, *et al.* Fabrication of SiC whisker reinforced laminated SiC/BN ceramics by spark plasma sintering. *Journal of Inorganic Materials*, 2002, **17**(6): 1220–1226.
- [11] HUANG Kang-Ming, LI Wei-Xin, RAO Ping-Gen, *et al.* Mechanical properties of $\text{Al}_2\text{O}_3/\text{Al}$ multilayer ceramics. *Journal of Synthetic Crystals*, 2009, **38**(1): 139–144.
- [12] HUANG Kang-Ming, LI Wei-Xin, RAO Ping-Gen, *et al.* Mechanical behavior mechanisms of $\text{Al}_2\text{O}_3/\text{Al}$ multilayer ceramics. *Journal of Synthetic Crystals*, 2009, **38**(2): 476–480.
- [13] Huang Kang-Ming, LI Wei-Xin, XIE Bing-Huan, *et al.* Preparation and mechanical properties of $\text{Al}_2\text{O}_3/\text{Al}$ laminated ceramic matrix composites. *Journal of Wuhan University of Technology (Materials Science)*, 2011, **26**(5): 891–896.
- [14] DENG Zhen-Yan, ZHANG Guo-Jun, Ando Motohide. Model analysis of multicrack mechanisms in ceramic/superplastic laminates. *Journal of American Ceramic Society*, 2002, **85**(7): 1793–1803.

Al_2O_3 /Steel-epoxy 层状复合材料的制备和性能

李伟信, 白明敏, 陆颖, 饶平根

(华南理工大学 材料学院, 广州 510640)

摘要: 采用环氧树脂胶黏剂作为粘结剂, 通过一种简单的模压方法, 在 5 MPa 压力下常温固化, 制备了一系列 Al_2O_3 /steel-epoxy 层状复合陶瓷材料。结果显示, Al_2O_3 /epoxy 界面和 steel/epoxy 界面结合紧密。相比于氧化铝薄片, Al_2O_3 /steel-epoxy 层状复合陶瓷材料强度差别不大, 但具有更高的断裂韧性、冲击韧性和断裂吸收能。裂纹扩展分析认为层状复合材料断裂韧性和能量吸收的提高主要得益于裂纹尖端钝化和捕获、裂纹桥连、层间脱粘和 steel-epoxy 层的塑性变形等机制。

关键词: 层状复合材料; 氧化铝; 界面; 钢丝-环氧树脂; 机械性能; 韧化机制

中图分类号: TQ174

文献标识码: A